

Effects of Sb content on microstructure and mechanical properties of Mg–6Zn–Y–Zr–xSb alloy

ZOU Chun-ming^{1,2,3}, ZHANG Yu-min², WANG Wei¹, WANG Hong-wei¹, WEI Zun-jie¹, FU Bin-guo¹

1. School of Materials Science and Engineering, Harbin Institute of Technology, Harbin 150001, China;

2. Center for Composite Materials, Harbin Institute of Technology, Harbin 150001, China;

3. Key Laboratory of Bionic Engineering of Ministry of Education, Jilin University, Changchun 130025, China

Received 10 May 2011; accepted 25 July 2011

Abstract: Effects of Sb content on microstructure and mechanical properties of Mg–6Zn–Y–Zr–xSb alloy were investigated by OM, SEM, XRD and mechanical property test. The results indicate that addition of Sb can break continuous network structure into particles in the interdendritic spaces, and with increasing Sb content, the volume fraction of these particles increases. The as-cast microstructure of the alloy with low content of Sb consists of α -Mg, Zn-rich phase, eutectic structure (α -Mg+*I*-phase) and YSb. With increasing Sb content, Mg₃Sb₂ and Mg₄Zn₇ phases appear, while *I*-phase disappears finally. The ultimate tensile strength and elongation increase first with the increase of Sb content, while the mechanical properties reduce at excessive Sb content.

Key words: Mg–6Zn–Y–Zr alloy; Sb addition; YSb; Mg₃Sb₂

1 Introduction

Mg–Zn–RE alloys possess a large potential in the field of mass reduction in aviation, spaceflight and auto appliances, and have good comprehensive mechanical and casting properties [1]. Especially, Mg–Zn–Y–Zr system alloys attract attention widely due to their low density, high strength and preferable age hardness [2–3]. Generally, there are three kinds of ternary equilibrium phases in Mg–Zn–Y–Zr systems, i.e. cubic Mg₁₂ZnY (*Z*-phase), Mg₃Zn₃Y₂ (*W*-phase) and icosahedral quasicrystal structure Mg₃Zn₆Y (*I*-phase) [4–5]. Among which, *I*-phase has many good properties such as high hardness thermal stability, low coefficient of friction, and low interfacial energy [6–7]. However, *I*-phase forms a network in the interdendritic spaces when the volume fraction of *I*-phase increases, which causes the mechanical properties of the alloys degrade greatly. So how to change the shape and distribution of microstructure of second phases gets more and more attention, and also becomes an urgent task.

Sb can produce thermally stable second phase constituents in Mg alloys under as-cast condition. According to the Mg–Sb binary phase diagram, the solubility of Sb in α -Mg is negligible, and thus the

intermetallic compound Mg₃Sb₂ can be formed in the system [8]. This is a highly stable phase with a high melting point, which is expected to enhance mechanical properties [9]. ALIZADEH and MAHMUDI [10] reported that Sb had a great effect on improving both room- and high-temperature mechanical properties of the Mg–4Zn alloy by refining the microstructure and formation of Mg₃Sb₂ particles. Recently, they found that the presence of Mg₃Sb₂ particles caused excellent stability, resulting in superior thermal stability of the Sb-containing Mg–4Zn alloys in comparison with the base alloy [11]. LIU et al [12] indicated that the tensile strength, elongation and hardness of the as-cast Mg–4Zn–Y alloy increased first with the increase of Sb content, but the mechanical properties reduced at excessive Sb content. Till now, there have not been reports on the effects of Sb additions on the as-cast microstructure and mechanical properties of Mg–Zn–Y–Zr alloy. Therefore, the aim of the present work is to study the effects of Sb addition on the as-cast microstructure and mechanical properties of a cast Mg–6Zn–Y–Zr alloy.

2 Experimental

The as-cast Mg–6Zn–Y–Zr–xSb alloys were made

by melting high-pure magnesium in an electric resistance furnace, and then 6.1% Zn, 2.0% Zr, 1.5% Y (mass fraction) and different contents of Sb were added under the protection of mixed SF₆ and CO₂ gas. After stirring the molten alloy and holding for 20–30 min at 740 °C, the molten alloys with different Sb contents were poured into sand mould with size of 110 mm×200 mm×12 mm. The chemical compositions of the alloys were determined by the inductively coupled plasma atomic emission spectrum (ICP-AES) apparatus and the result is listed in Table 1.

Table 1 Chemical composition of test alloys (mass fraction, %)

Nominal alloy	Zn	Y	Zr	Sb	Mg
Mg–6Zn–Y–Zr	5.91	0.85	0.62	–	Bal.
Mg–6Zn–Y–Zr–0.015Sb	5.91	0.80	0.61	0.015	Bal.
Mg–6Zn–Y–Zr–0.04Sb	5.85	0.70	0.63	0.042	Bal.
Mg–6Zn–Y–Zr–0.07Sb	5.92	0.78	0.59	0.072	Bal.
Mg–6Zn–Y–Zr–0.8Sb	5.85	0.77	0.61	0.83	Bal.
Mg–6Zn–Y–Zr–2Sb	5.92	0.77	0.58	2.02	Bal.

The microstructures of the as-cast alloys were examined by means of optical microscopy (OLYMPUS–GX71) and scanning electron microscopy (SEM, Hitachi S–4700) with energy dispersive spectroscopy (EDS). Alloys were etched with an etchant of 2 mL nitric acid and 98 mL ethanol. Phase analysis was determined by D/Max 2400 X-ray diffractometer (XRD). The tensile bars with size of 25 mm×6 mm×2 mm were machined from the alloys. Tensile experiments were conducted on the INSTRON 5569 testing machine at a constant strain rate of $1 \times 10^{-3} \text{ s}^{-1}$ at room temperature.

3 Results and discussion

3.1 Microstructural evolution

The optical microstructures of the as-cast alloys with different additions of Sb are shown in Fig. 1. As can be seen, the dendritic structure of the Mg–6Zn–Y–Zr alloy is generally coarsened after the addition of Sb, and the achieved coarsening is more pronounced at 0.042% Sb. Increasing Sb content to 2.02%, however, leads to the refining of dendritic structure, though the grain size is still coarser than that of Mg–6Zn–Y–Zr alloy. When the Sb content is more than 0.042%, the initial network structure is broken and a rather uniform distribution of second phases is obtained.

The XRD patterns shown in Fig. 2 indicate that α -Mg, Mg₃Zn₃Y₂ (*W*-phase) and Mg₃Zn₆Y (*I*-phase) are the only constituents in the Mg–6Zn–Y–Zr alloy. These phases have also been reported to exist in the

microstructure of an as-cast Mg–Zn–Y–Zr alloy [4]. In the Sb-containing alloys, however, some new peaks corresponding to Mg₃Sb₂ appear in the patterns. The intensity of these peaks increases with increasing Sb content of the alloys. The relatively high-magnification micrographs of the alloys are shown in Fig. 3. The microstructure of the Mg–6Zn–Y–Zr alloy consists of primary α -Mg matrix, grain boundary phase and lamellar eutectic structure, as shown in Fig. 3(a). EDS analysis of the eutectic phase indicates an average composition of 69.5% Mg, 4.3% Y and 26.2% Zn (molar fraction) for the eutectic phase. Due to the very small size of the Mg–Zn–Y particles in the eutectic structure and grain boundary, it is not possible to determine the exact composition of these particles. However, according to the XRD results, these particles are determined to be Mg₃Zn₆Y compound, and thus the lamellar eutectic structure consists of α -Mg+Mg₃Zn₆Y. Besides Mg₃Zn₆Y, there is a little amount of Mg₃Zn₃Y₂ in the grain boundary according to the XRD results and Ref. [13].

In the Sb-containing alloys, however, the volume fraction of eutectic structure containing *I*-phase decreases as the Sb content of the alloy increases until it disappears (Figs. 3(b)–(d)). In Mg–6Zn–Y–Zr–2Sb alloy, the eutectic structure changes into α -Mg+Mg₄Zn₇ according to the SEM observation and XRD results. At the same time, some particles are formed (Figs. 3(b)–(d)). As can be observed, the size and volume fraction of these particles increase as the Sb content of the alloy increases. These particles are three kinds of phases containing different elements according to EDS or XRD results. Block phase contains an average composition of 54.9% Y and 45.1% Sb (molar fraction), which is close to the composition of YSb by EDS results. It has also been reported to exist in the as-cast microstructure of an Mg–4Zn–Y–Sb alloy, and it is dealt with as YSb [12]. Due to the small amount of this phase, it can not be detected by XRD or determined exactly. Rod shape particles (see Fig. 3(f)) consist of Mg and Sb, which have an average composition of 76.5% Mg and 23.5% Sb (mass fraction) according to EDS results, close to the composition of Mg₃Sb₂ compound according to the Mg–Sb phase diagram [8]. The XRD results also support this conclusion. As discussed later, this intermetallic compound would affect the mechanical behavior of the materials. The third type particles distribute in the interdendritic spaces, where no other elements but Mg and Zn are detected by EDS. It is demonstrated that a supersaturated solid solution of Zn in Mg, with a composition of approximately 6.5% Zn and 93.5% Mg (mass fraction), exists in interdendritic spaces. All these particles are formed inside this supersaturated solid solution of Zn, and so it is a Zn-rich phase [10].

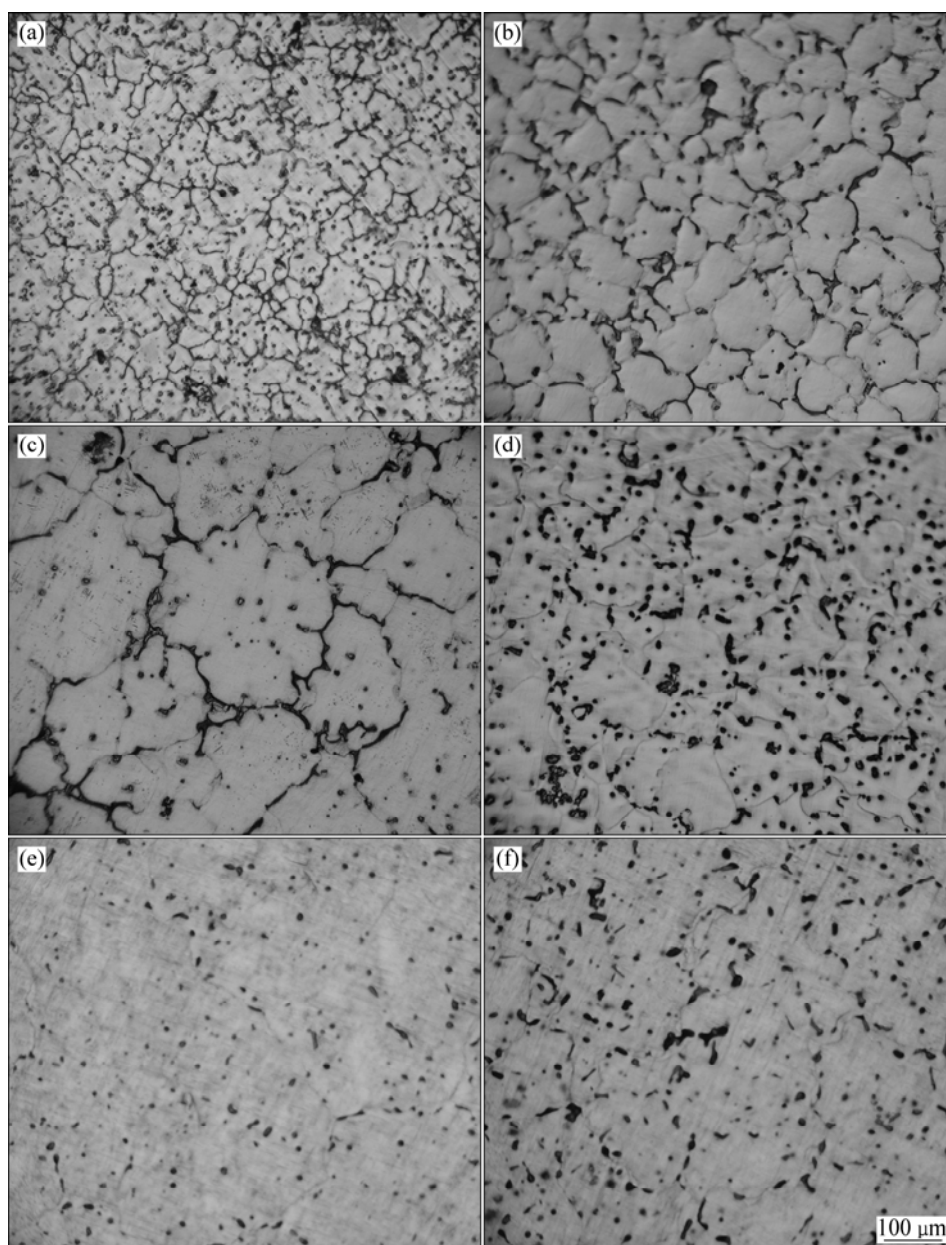


Fig. 1 Optical micrographs of as-cast alloys: (a) Mg-6Zn-Y-Zr; (b) Mg-6Zn-Y-Zr-0.015Sb; (c) Mg-6Zn-Y-Zr-0.04Sb; (d) Mg-6Zn-Y-Zr-0.07Sb; (e) Mg-6Zn-Y-Zr-0.08Sb; (f) Mg-6Zn-Y-Zr-2Sb

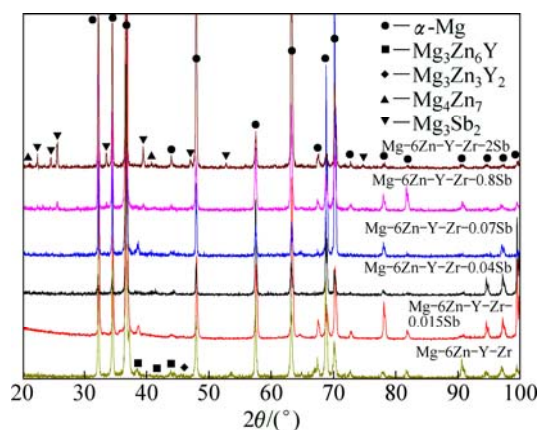


Fig. 2 XRD patterns of as-cast Mg-6Zn-Y-Zr-xSb alloys

Table 2 lists the phase composition in Mg-6Zn-Y-Zr-xSb alloy according to the above analysis. With all contents of Sb addition, α -Mg and Zn-rich phase exist in Mg-6Zn-Y-Zr-xSb alloy. As Sb is added into the alloy, even with a small amount, $\text{Mg}_3\text{Zn}_3\text{Y}_2$ phase disappears. At the same time, YSb and Mg_3Sb_2 phases are formed in the alloy. With increasing Sb content of the alloy, the volume fractions of both phases increase, while the volume fraction of $\text{Mg}_3\text{Zn}_6\text{Y}$ phase decreases until these phases disappear, at last Mg_4Zn_7 phase begins to form in the shape of lamellar eutectic structure. Figure 4 shows the SEM image of eutectic structure (α -Mg+ Mg_4Zn_7) on Mg_3Sb_2 phase. During the last stage of solidification, the content of melt alloy fits the eutectic

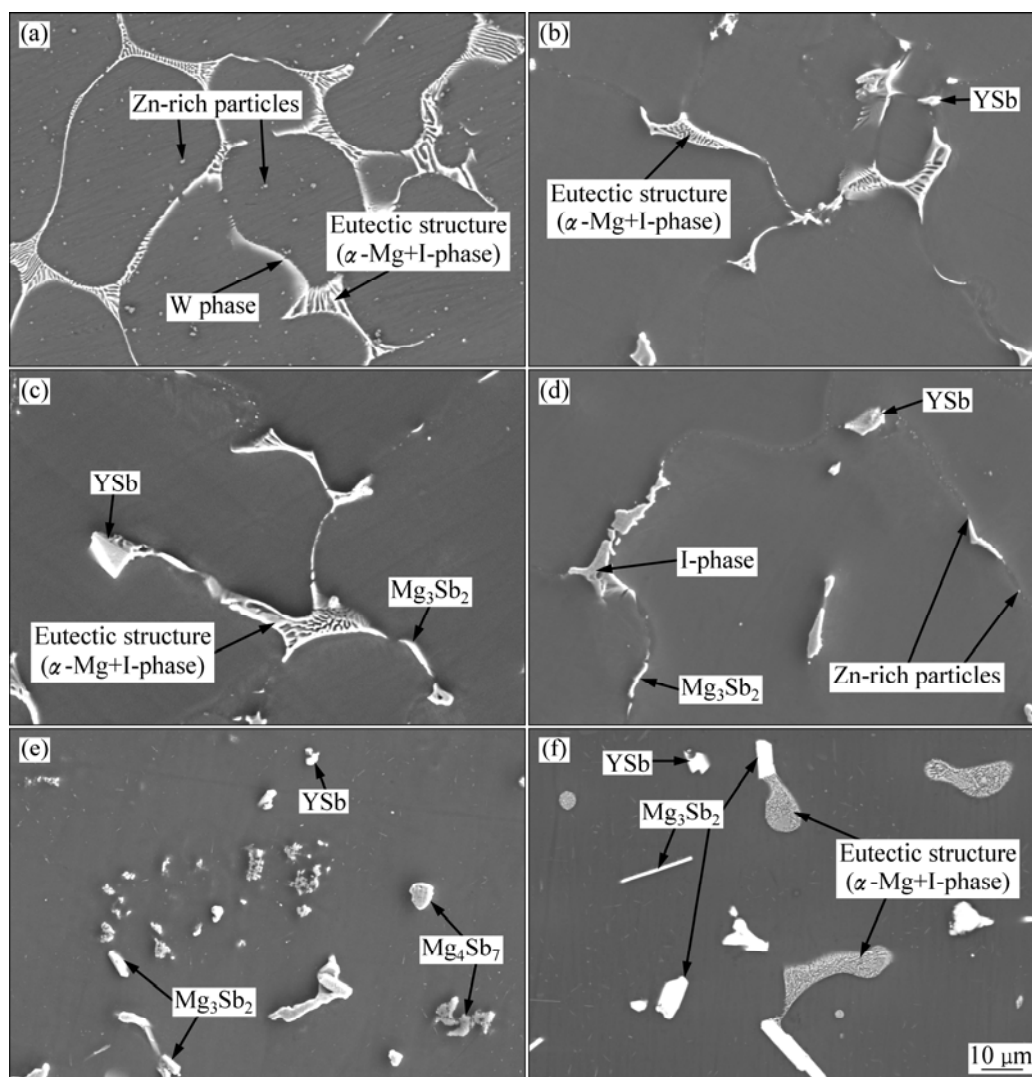


Fig. 3 SEM micrographs of alloys showing intermetallic particles: (a) Mg-6Zn-Y-Zr; (b) Mg-6Zn-Y-Zr-0.015Sb; (c) Mg-6Zn-Y-Zr-0.04Sb; (d) Mg-6Zn-Y-Zr-0.07Sb; (e) Mg-6Zn-Y-Zr-0.8Sb; (f) Mg-6Zn-Y-Zr-2Sb

Table 2 Microstructure of Mg-6Zn-Y-Zr-xSb alloy

Sb content/%	Microstructure
0	α -Mg+Zn-rich phase+ (α -Mg+Mg ₃ Zn ₆ Y)+Mg ₃ Zn ₃ Y ₂
0.015	α -Mg+Zn-rich phase+ (α -Mg+Mg ₃ Zn ₆ Y)+YSb
0.042	α -Mg+Zn-rich phase+ Mg ₃ Zn ₆ Y+YSb+Mg ₃ Sb ₂
0.072	α -Mg+Zn-rich phase+ Mg ₃ Zn ₆ Y+YSb+Mg ₃ Sb ₂
0.83	α -Mg+Zn-rich phase+ Mg ₄ Zn ₇ +YSb+Mg ₃ Sb ₂
2.02	α -Mg+Zn-rich phase+ (α -Mg+Mg ₄ Zn ₇)+YSb+Mg ₃ Sb ₂

reaction, and if the liquid is just contacted with Mg₃Sb₂ particles, Mg₃Sb₂ particles may act as heterogeneous nucleation sites for Mg₄Zn₇. The similar phenomenon was observed that Sb-containing phases can also be the substrates for eutectic structure in Mg-4Zn alloy [10].

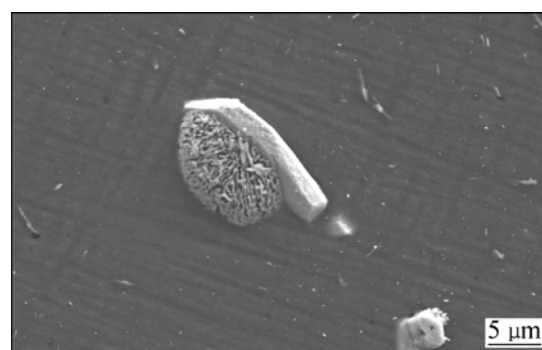


Fig. 4 SEM image of eutectic structure (α -Mg+Mg₄Zn₇) grown on Mg₃Sb₂ phase in Mg-6Zn-Y-Zr-2Sb alloy

The hindering of α -Mg grain growth during solidification can be considered a possible grain refinement mechanism. The role of Sb addition into alloy is consuming Y to produce YSb and Mg_3Sb_2 firstly, when Sb content is high, Y for $\text{Mg}_3\text{Zn}_6\text{Y}$ phase is also plundered, and just only Mg_4Zn_7 can be formed. Due to the high melting point (1 245 °C) of Mg_3Sb_2 and the high affinity of Sb to Mg, Mg_3Sb_2 particles may form before Mg grains and Mg_4Zn_7 particles during solidification [10]. Mg_3Sb_2 particles may stand at the liquid-solid interface, hindering the grain growth of α -Mg during solidification, and when the mount of Mg_3Sb_2 particles is large, it can refine the grain structure. However, due to a lot of Y is consumed, the refinement action of Y is weakened, so the size of grain is still larger than that of the base alloy (Mg-6Zn-Y-Zr).

In addition to the presence of second-phase particles which hinder the grain growth of α -Mg, the grain refinement action of Sb addition has a pronounced impact on the enhancement of mechanical properties of the cast alloys. The grain refining effect of Sb on cast magnesium alloys has attracted some attentions. A little amount of Sb addition to the Mg-4Zn alloy has resulted in significant refinement of the as-cast microstructure [10]. The addition of Sb to AZ91 [14] and Mg-9Al alloys [15] also results in microstructural refinement. In the present work, the addition of Sb results in grain coarsening compared with the base alloy (Mg-6Zn-Y-Zr). In the discussion of the grain refinement mechanism of Sb addition to the Mg-4Zn alloy, ALIZADEH and MAHMUDI [10] calculated the misfits between α -Mg and Mg_3Sb_2 , with a misfit value of 29%, which did not satisfy the criterion (misfit value should be less than 15%) to act as nucleating sites for Mg grains [10]. Thus, Mg_3Sb_2 does not act as nucleating sites for Mg grains, the hindering of α -Mg grain growth should be the main grain refinement mechanism of Sb addition.

3.2 Mechanical properties

The stress—strain curves are shown in Fig. 5. It shows that when the Sb content increases from 0 to 0.072%, the ultimate tensile strength and elongation improve from 180 MPa and 2.7% to 220 MPa and 12.2%, respectively. However, with further increasing the Sb content, the ultimate tensile strength and elongation of the alloys degrade greatly. When the Sb content of the alloy reaches to 2.02%, the ultimate tensile strength and the elongation of alloys decrease to 126 MPa and 5.1%, respectively. The relationship between the Sb content and the mechanical properties for alloys is summarized, as listed in Table 3. It is found that the yield stresses of Sb-containing alloys are lower than that of the alloy without Sb addition.

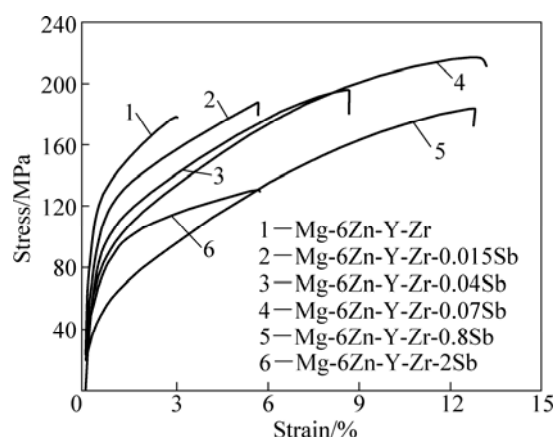


Fig. 5 Stress—strain curves of Mg-6Zn-Y-Zr-xSb alloy

Table 3 Mechanical properties of Mg-6Zn-Y-Zr-xSb alloys

Sb content/%	Ultimate tensile strength/MPa	Elongation/%	Yield strength/MPa
—	180	2.7	115
0.015	188	4.9	95
0.042	197	7.5	90
0.072	220	12.2	75
0.83	185	11.0	51
2.02	126	5.1	72

The tensile results show that the variation of Sb content can influence the mechanical properties of the as-cast Mg-6Zn-Y-Zr-xSb alloys greatly. Based on the microstructure observations and XRD analysis, the main reason can be ascribed to two aspects, i.e. grain size and evolution of the second phases. Generally, the yield strength of the alloys varies with the grain size following the Hall-Petch relationship. According to this relationship, the yield strength of the alloy with a smaller grain size should be higher. The grain size of Mg-6Zn-Y-Zr-0.04Sb alloy is the largest. However, the tensile results show that the yield strength of Mg-6Zn-Y-Zr-0.04Sb alloy is not the lowest, whereas the yield strength of the alloy is higher than most of Sb-containing alloys, which strongly disobeys the Hall-Petch relationship. Therefore, the influence of the relationship between the Sb addition and microstructure on the mechanical properties must be deeply investigated to explain this abnormal phenomenon.

When the Sb content is 0.015%, Sb just consumes a little Y in the alloy, and the refinement action of Y remains. So the grain coarsening is limited and the yield strength degrades slowly (see Figs. 1(a), (b) and Fig. 5). At the same time, due to the Sb addition, W -phase

disappears and the network structure is partly broken, which enhances the ultimate tensile strength and the elongation. When the Sb content is 0.042%, Sb consumes a lot of Y, a small quantity of YSb and Mg_3Sb_2 are formed in the alloy, and the refinement action of Y is limited, while the refinement action of the Mg_3Sb_2 does not work enough due to the small volume fraction. So the grain coarsens and the yield strength degrades (see Figs. 1(c), 2(c) and 5). At the same time, due to the Sb addition, the network structure in the alloy is partly broken, which enhances the ultimate tensile strength and the elongation. Compared with the alloy with Sb content of 0.042%, the refinement action of the Mg_3Sb_2 begins to work in the alloy with Sb content of 0.072%, and the grain size begins to decrease although it is still larger than that of Mg–6Zn–Y–Zr alloy. At this content of Sb, the network structure is broken drastically and *I*-phase is still the main enhanced phase, so the ultimate tensile strength and the elongation increase greatly. With increasing content of Sb, the volume fraction of *I*-phase decreases gradually, and at the same time the amount of Mg_4Zn_7 increases gradually (see Figs. 1(e)–(f) and 2(e)–(f). It was reported that *I*-phase is the best strengthening phase in Mg–Zn–Y–Zr alloy, and enhances Mg alloys more effectively than Mg_4Zn_7 or Mg_3Sb_2 [13]. So the disappearance of *I*-phase results in the decrease of mechanical properties.

To sum up the above arguments, the role of Sb addition is to break the continuous network structure in the interdendritic spaces and enhance the mechanical properties of the alloy. However, it can weak the refinement of Y element, suggesting the content of Sb added into Mg–Zn–Y–Zr alloys should be just the right amount to obtain enough *I*-phase to be the main enhanced phase.

4 Conclusions

1) The addition of Sb can break the continuous network structure into particles in the interdendritic spaces, and with increasing Sb content, the volume fraction of these particles increases.

2) The as-cast microstructure of the alloy with low content of Sb consists of α -Mg, eutectic structure (α -Mg+*I*-phase) and YSb. With increasing Sb content, Mg_3Sb_2 phase and Mg_4Zn_7 appear, while *I*-phase disappears finally.

3) The ultimate tensile strength and the elongation increase first with the increase of Sb content, while the mechanical properties decrease at the excessive Sb content.

References

- [1] ZHANG Ya, ZENG Xiao-qing, LU Chen, DING Wen-jiang. Deformation behavior and dynamic recrystallization of a Mg–Zn–Y–Zr alloy [J]. Materials Science and Engineering A, 2006, 428: 91–97.
- [2] XU D K, TANG W N, LIU L, XU Y B, HAN E H. Effect of W-phase on the mechanical properties of as-cast Mg–Zn–Y–Zr alloys[J]. Journal of Alloys and Compounds, 2008, 461(1–2): 248–252.
- [3] XU D K, LIU L, XU Y B, HAN E H. The fatigue behavior of *I*-phase containing as-cast Mg–Zn–Y–Zr alloy [J]. Acta Materialia, 2008, 56(1–2): 985–994.
- [4] XU D K, TANG W N, LIU L, XU Y B, HAN E H. Effect of Y concentration on the microstructure and mechanical properties of as-cast Mg–Zn–Y–Zr alloys [J]. Journal of Alloys and Compounds, 2007, 432(1–2): 129–134.
- [5] LUO Zhi-ping, ZHANG Shao-qing, TANG Ya-li, ZHAO Dong-shan. Quasicrystals in as-cast Mg–Zn–RE alloys [J]. Scr Metall Mater, 1993, 28(12): 1513–1518.
- [6] PIERCE F S, POON S J, GUO Q. Electron localization in metallic quasicrystals [J]. Science, 1993, 261(5122): 737–739.
- [7] LUO Z P, ZHANG S Q, TANG Y L, ZHAO D S. On the stable quasicrystals in slowly cooled Mg–Zn–Y alloys [J]. Scr Metall Mater, 1995, 32(9): 1411–1416.
- [8] PALIWAL M, JUNG I H. Thermodynamic modeling of the Mg–Bi and Mg–Sb binary systems and short-range-ordering behavior of the liquid solutions [J]. CALPHAD: Computer Coupling of Phase Diagrams and Thermochemistry, 2009, 33(4): 744–754.
- [9] YUAN Guang-yin, SUN Yang-shan, DING Wen-jiang. Effects of Sb addition on the microstructure and mechanical properties of AZ91 magnesium alloy [J]. Scripta Mater, 2000, 43(11): 1009–1013.
- [10] ALIZADEH R, MAHMUDI R. Evaluating high-temperature mechanical behavior of cast Mg–4Zn–xSb magnesium alloys by shear punch testing [J]. Materials Science and Engineering A, 2010, 527(16–17): 3975–3983.
- [11] ALIZADEH R, MAHMUDI R. Effect of Sb additions on the microstructural stability and mechanical properties of cast Mg–4Zn alloy [J]. Materials Science and Engineering A, 2010, 527(20): 5312–5317.
- [12] LIU Xi-liang, LIU Zi-li, YANG Ming. Effects of Sb content on microstructure and properties of Mg–4Zn–Y alloy [J]. Hot Working Technology, 2010, 39(4): 25–27. (in Chinese)
- [13] HUANG Z H, LIANG S M, CHEN R S, HAN E H. Solidification pathways and constituent phases of Mg–Zn–Y–Zr alloys [J]. Journal of Alloys and Compounds, 2009, 468(1–2): 170–178.
- [14] SRINIVASAN A, SWAMINATHAN J, PILLAI U T S, KRISHNA GUGULOTH, PAI B C. Effect of combined addition of Si and Sb on the microstructure and creep properties of AZ91 magnesium alloy [J]. Materials Science and Engineering A, 2008, 485(1–2): 86–91.
- [15] YUAN Guang-yin, SUN Yang-shan, WANG Zhen. Effect of antimony on microstructure and mechanical properties of Mg–9Al based alloy [J]. The Chinese Journal of Nonferrous Metals, 1999, 9(4): 779–784. (in Chinese)

Sb 含量对 Mg-6Zn-Y-Zr-xSb 合金组织与性能的影响

邹鹤鸣^{1,2,3}, 张宇民², 汪 伟¹, 王宏伟¹, 魏尊杰¹, 付彬国¹

1. 哈尔滨工业大学 材料科学与工程学院, 哈尔滨 150001;
2. 哈尔滨工业大学 复合材料研究所, 哈尔滨 150001;
3. 吉林大学 工程仿生教育部重点实验室, 长春 130025

摘 要: 利用 OM、SEM、XRD 及力学性能测试, 研究 Sb 含量对 Mg-6Zn-Y-Zr-xSb 合金铸态组织及性能的影响。结果表明: 添加 Sb 可以使晶界处网状连续组织变为颗粒状, 并且随着 Sb 含量增加, 颗粒的体积分数增加。低 Sb 含量合金的铸造组织由 α -Mg、富锌相、共晶组织(α -Mg+I 相)和 YSb 组成; 随着 Sb 含量的增加, I 相逐渐消失, Mg_3Sb_2 和二元共晶 Mg_4Zn_7 开始出现。起初合金的拉伸强度和延伸率随 Sb 含量的增加而提高, 而当 Sb 含量过大时, 合金的综合力学性能下降。

关键词: Mg-6Zn-Y-Zr 合金; Sb 添加; YSb; Mg_3Sb_2

(Edited by FANG Jing-hua)